Fracture Analysis of Electronic IC Package in Reflow Soldering Process

Ji Hyuck Yang
Currently, Hyundai Motor Company,
772-1, Jangduk-Dong, Whasung-Si, Gyunggi-Do, 445-706, Korea
Kang Yong Lee*
School of Mechanical Engineering, Yonsei University,
SinchonDong, SeodaemoonGu, Seoul 120-749, Korea
Taek Sung Lee
Department of Mechanical Design Engineering, Korea Polytechnic University,
Shiheung City, Kyungki-do, 429-450, Korea
She-Xu Zhao
Department of Engineering Mechanics, Shanghai Jiaotong University,
Shanghai 200240, China

The purposes of the paper are to analyze the fracture phenomenon by delamination and cracking when the encapsulant of plastic IC package with polyimide coating shows viscoelastic behavior under hygrothermal loading in the IR soldering process and to suggest more reliable design conditions by the approaches of stress analysis and fracture mechanics. The model is the plastic SOJ package with the polyimide coating surrounding chip and dimpled diepad. On the package without cracks, the optimum position and thickness of polyimide coating to decrease the maximum differences of strains at the bonding surfaces of parts of the package are studied. For the model delaminated fully between the chip and the dimpled diepad, C(t)-integral values are calculated for the various design variables. Finally, the optimal values of design variables to depress the delamination and crack growth in the plastic IC package are obtained.

Key Words : Plastic IC Package, Polyimide Coating, Viscoelastic Analysis, C(t)-integral Value, Hygrothermal Loading

1. Introduction

Because a plastic IC package reaches high temperature above 200℃ during reflow soldering process, the thermal stress occurs due to the mismatch of thermal expansion coefficients between the parts of the package. The thermal stress causes the delamination between the parts and the cracking phenomenon results (Hattori et al., 1989). Also, the epoxy molding compound (EMC) used as a packaging material absorbs the moisture in the atmosphere, which produces vapor pressure during surface mounting process. The vapor pressure due to the vaporization of the moisture may cause the popcorn failure (Adachi et al., 1993; Kawamura et al., 1993).

Until now, the vapor pressure due to the moisture has been assumed as the saturated vapor pressure without consideration of the hygroscopic time and condition (Kawamura et al., 1993), and the conventional failure criterion based on bending or shear strength has been considered (Glaser and Juaire, 1989; Kornblum and Glaser,

* Corresponding Author,
E-mail : KYL2813@yahoo.co.kr
TEL : +82-2-2123-2813; **FAX** : +82-2-312-2159
School of Mechanical Engineering, Yonsei University, SinchonDong, SeodaemoonGu, Seoul 120-749, Korea.
(Manuscript **Received** February 12, 2003; **Revised** December 22, 2003)

1989). But, to get the more reliable results, the vapor pressure must be calculated with the variation of time for the hygroscopic time and condition and the fracture criterion based on fracture mechanics should be applied (Sauber et al., 1994 ; Kuo et al. 1996). Stevens et al.(1990) used J-integral as the fracture mechanics parameter to carry out the crack analysis for the glass seal of the thin layer surrounding lead frame in IC package.

As vapor pressure is influenced by the content of the absorbed moisture, the analytical solutions for the vapor pressure with consideration of the moisture content are necessary but rare (Kitano et al., 1988 ; Kitano et al., 1989). Until now it has been assumed that at the delaminated space the saturated vapor pressure occurs during the reflow soldering process (Tay and Lin, 1996), despite that the moisture to be absorbed into the package should be obtained from the moisture diffusion theory. Nguyen (1993) reported that the ionic impurities in the moisture absorbed into IC package could exist because the package contains the phthalate ester and plasticizers etc.. Fukuzawa et al.(1985) reported that the free Cl ion in the absorbed moisture corrodes aluminum. In addition that these impurities corrode the circuit of IC package, they lower the saturated vapor pressure according to Raoult's law. Therefore, though the humidity in the delaminated space is lower than that in the outer space of the package, the condensed water can exist in the delaminated space due to the drop of the saturated vapor pressure of the contaminated water. Consequently, the quantity of the moisture absorbed into the delaminated gap depends on the hygroscopic time, the thickness of package and the quantity of impurities. Recently, Lee and Lee (1999) evaluated the variation of vapor pressure during the IR soldering process with consideration of them.

EMC experiences a high temperature above glass transition temperature, Tg, during reflow soldering process. Kenner et al.(1997) reported that EMC shows viscoelastic behavior in high temperature above glass transition temperature. Yang and Lee (2000) made the crack analysis of IC package with consideration of the viscoelasticity.

The package model with polyimide coating has been shown to reduce the stress in IC package (Romer and Pape, 1989 ; Takeuchi et al., 1990 ; Omi et al., 1990). Romer and Pape (1989) showed that the compressive stress increases as the thickness of polyimide coating increases. Takuechi et al.(1990) presented the experimental results that the coating of various polyimides on the upper surface of IC chip has a good adhesion property and can suppress the occurrence of package cracks. Omi et al.(1990) reported that the polyimide coating on the back side of the diepad can depress the crack at the corner of diepad.

The previous research has not considered the viscoelastic behavior of EMC in the package with polyimide coating. Therefore, in this paper, we study the viscoelastic behavior of the plastic IC package with the polyimide coating under thermal loading and mechanical loading varied with the quantity of impurities, and the effect of polyimide coating on the stress and fracture of the package. Finally, we show the values of design parameters to depress the crack growth in the package with polyimide coating by calculating C(t)-integral value as a creep fracture mechanics parameter.

2. Viscoelastic Temperature and Thermal Stress Analysis for the Model with Polyimide Coating in the Case of No Crack

The package is SOJ(small outline J-lead) type with polyimide coating as shown in Fig. 1. The software used for the finite element analysis is ABAQUS. The element used to obtain the temperature distribution is a two-dimensional quadrilateral isoparametric and one for stress analysis is a two-dimensional plain strain. The 2-D FE model is composed of half the package because it is symmetric. The quadratic shape function is used. The number of elements is 887 which is shown to be enough for the numerical accuracy. The FE meshes are identical for the calculations of the temperature and stress distributions (same

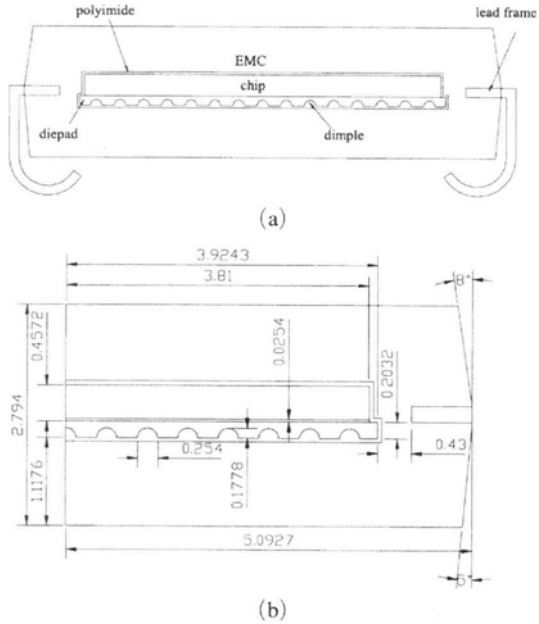

Fig. 1 SOJ plastic package with polyimide coating

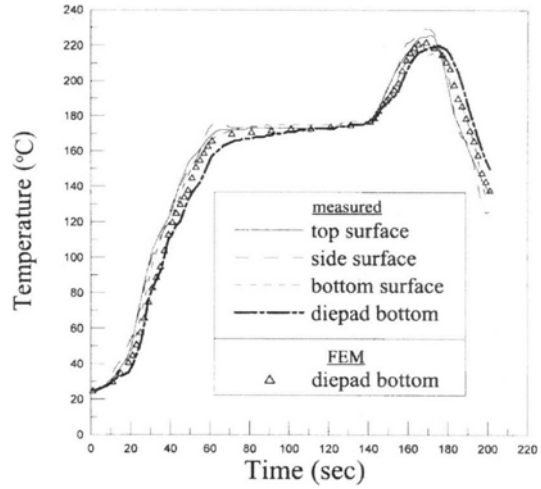

Fig. 2 Comparison with the measured and calculated temperature profiles at the boundary surfaces of the IC package during the reflow soldering process

as the model of no crack in Fig. 9 except the neighborhood of the crack tip).

For the temperature boundary conditions the temperatures at the top, side, and bottom surfaces of the package are measured using the K-type thermocouple (0.1 mm diameter). During the reflow soldering process, the changes of the temperature at the boundary are measured. To check the reliability of the finite element simulation the temperature at the diepad bottom is also measured. For the measurement of the temperature at diepad bottom, a hole of about 1.5 mm from the bottom of the package to diepad is made and the thermocouple is inserted and the hole is filled up with the epoxy of the same kind of EMC. After the temperature profiles are measured three times, the values for each position are averaged.

The measured temperature profiles are shown in Fig. 2. By using the temperature profiles at the top, side and bottom surfaces of the package, the temperature distribution of the whole package is obtained by the FE analysis. In the calculation of the temperature distribution, it is assumed to be an adiabatic condition on the symmetric surface. Fig. 2 also shows that the largest difference between the measured temperature profile and the calculated one at the diepad bottom is within 5 percent.

Material properties for temperature and stress analysis are shown in Table 1, where α_1 and α_2 are the thermal expansion coefficients below and above glass transition temperature, Tg, respectively. It is assumed that polyimide shows an elastic behavior because the temperature in the reflow soldering process doesn't exceed the glass transition temperature of polyimide and the heating time is short.

The temperature distribution of each node at the instant becomes the input data for calculating the thermal stress in the package. The stress free temperature is assumed 170℃, which is the molding temperature of the IC package. The boundary conditions for stress analysis are that the symmetric surface is fixed in the x-direction and the bottom corner node of symmetric surface is fixed in the x and y-directions.

To know the effect of the polyimide coating on the delamination in the package, we set up three model cases as shown in Fig. 3. The thickness of polyimide coating layer is 0.0254 mm (1 mil). With comparing the differences between the strains at the above element and the bottom one

Table 2 Material properties of IC package (Lee and Lee, 1999 ; Yong and Lee, 2000 ; Romer and Pape, 1989)

	Lead-frame		Chip (Si)	EMC	Adhesive (Ag-epoxy)	Coating (polyimide)
	alloy42	copper				
Specific heat (J/kg ℃)	502.4	383	699	1050	0.234	1100
Conductivity coefficient (W/m ℃)	14.65	190	148	0.735	374	0.2
Density (kg/m^3)	8.1×10^3	8.9×10^3	2.33×10^3	1.9×10^3	1.05×10^4	1.42×10^3
Thermal expansion coefficicient (/℃)	0.45×10^{-5}	1.7×10^{-5}	0.26×10^{-5}	a_1 : 1.0×10^{-5} a_2 : 4.5×10^{-5}	a_1 : 4.9×10^{-5} a_1 : 2.4×10^{-4}	2.0×10^{-5}
Young's modulus (N/m^2)	1.45×10^{11}	1.17×10^{11}	1.88×10^{11}	2.45×10^{10}(25℃) 2.0×10^{10}(70℃) 1.0×10^{10}(150℃) 1.0×10^{9}(215℃)	1.2×10^9 (23℃)	3.5×10^9
Poisson's ratio	0.3	0.35	0.28	0.23	0.3	0.3
Glass transition temperature (℃)		•	•	133-145	36	385

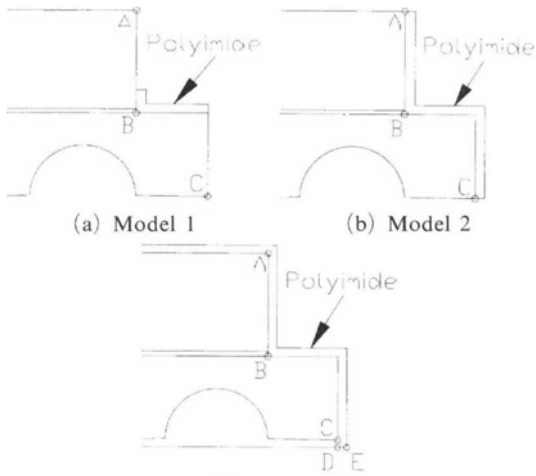

Fig. 3 IC package models with different polyimide coating

on the interfaces, it is found that the locations of large differences of strains are A, B, and C positions as shown in Fig. 3 and the values are shown in Table 2 with those of the case without polyimide coating.

Table 2 shows that the differences of the strains at the interface for the case with polyimide coating are smaller than those without polyimide coating. In the research on the properties of various polyimide coating and the effect of the coating on the crack occurrence and interface adhesion, Takeuchi et al.(1990) reported that high heat resistance, high mechanical strength, stress relaxation property such as low elastic modulus are needed on the view point of stress relaxation and polyimide is mostly suitable. Therefore, our results that polyimide coating decreases the differences of the strains at the interface are reasonable. Table 2 also shows the differences of strains at the interface between the parts are smallest in case of "Model 3". Therefore, we select "Model 3" as the polyimide coating model to reduce the possibility of the delamination and microcracking.

Table 2 Change of the differences of strains at the different locations for the models with and without polyimide coating

	Location	With polyimide coating			Without polyimide coating
		Model 1	Model 2	Model 3	
$\Delta\gamma_{xy}$	A	0.06494	0.05844	0.02880	0.06456
	B	0.05266	0.05340	0.05417	0.06779
	C	0.06520	0.05428	0.2704	0.06471
$\Delta\varepsilon_y$	A	0.01531	0.01947	0.00203	0.01529
	B	0.03506	0.03507	0.02931	0.03253
	C	0.01581	0.01973	0.00517	0.01709

Table 3 Change of the differences of strains at the different locations with the thickness of polyimide coating in "Model 3"

	Position / Thickness (mm)	A	B	C
$\Delta\gamma_{xy}$	0.0254	0.02880	0.05417	0.02704
	0.0381	0.02762	0.03072	0.02670
	0.0508	0.02567	0.02631	0.02508
	0.0635	0.02544	0.04296	0.02358
	0.0762	0.02448	0.03885	0.02221
$\Delta\varepsilon_y$	0.0254	0.00203	0.02931	0.00517
	0.0381	0.00291	0.02773	0.00386
	0.0508	0.00327	0.02598	0.00401
	0.0635	0.00358	0.02626	0.00428
	0.0762	0.00383	0.02642	0.00433

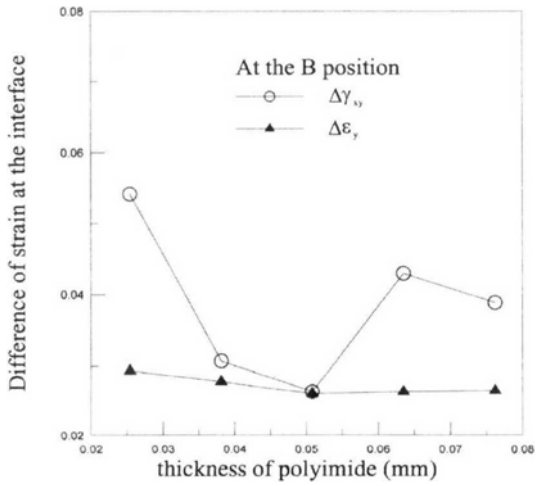

Fig. 4 Change of the difference of strain at the interface with the thickness of polyimide coating at the B position shown in Fig. 3

In that model, we present the change of the differences of strains at the interface with the thickness of polyimide coating in Table 3. The location at which maximum differences of strains occur is the "B" position regardless of the thickness of polyimide coating. When the thickness of polyimide coating changes between 0.0254 mm and 0.0762 mm, the least values of $\Delta\gamma_{xy}$ and $\Delta\varepsilon_y$ at "B" are gotten in the case of the thickness of 0.0508 mm (2 mil). Especially, the differences of strains at the "B" position are shown in Fig. 4. Therefore, from now on, the thickness of polyimide coating in "Model 3" is fixed to be 0.0508 mm.

3. Analysis for Moisture Absorption and Vapor Pressure

The delamination model is shown in Fig. 5,

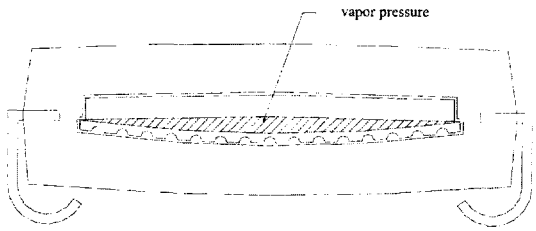

Fig. 5 The model for the moisture absorption analysis and the calculation of the vapor pressure

which is the case delaminated fully between chip and diepad and it is caused from the result that the differences of strains are largest at the "B" position between chip and diepad according to the above stress analysis.

To consider the effect of the impurities on the saturated vapor pressure, we define a contamination factor, f, in the form,

$$f \equiv \frac{p_s}{P_{s(d,w.)}} \tag{1}$$

where p_s is the saturated vapor pressure of the contaminated water and $P_{s(d,w.)}$ is the saturated vapor pressure of the distilled water.

The moisture concentration (C) absorbed into EMC which is dependent on the time (t) and the distance from the diepad (x) is described by Fick's second law,

$$\frac{\partial C}{\partial t} = D \frac{\partial^2 C}{\partial x^2} \tag{2}$$

$$C(t=0) = C_0(x) \tag{3}$$

$$C(x=0) = pS \tag{4}$$

$$C(x=h) = \rho p_s S \tag{5}$$

where D is the diffusion coefficient of moisture (mm^2/s) and assumed to be independent of moisture content, C_0 is the initial distribution of moisture concentration (mg/mm^3), p is the vapor pressure (MPa) in the delaminated space, p_s is the saturated vapor pressure (MPa), ρ is the relative humidity of atmosphere, S is the solution coefficient ($mg/mm^3/MPa$), and h is the distance from the diepad to the boundary surface of EMC. The diffusion coefficient of moisture D and the solution coefficient S are described by the Arrhenius-type expressions (Kitano et al., 1988). Here, in EMC D_0 is $4.26\times10^{-3}\ mm^2/s$, E_D is 2.41×10^4 J/mol, S_0 is $2.52\times10^{-6}\ mg/mm^3/MPa$, and E_S is -3.27×10^4 J/mol, and in polyimide D_0 is $3.156\ mm^2/s$, E_D is 4.20×10^4 J/mol, S_0 is $2.958\times10^{-7}\ mg/mm^3/MPa$, and E_S is -4.32×10^4 J/mol (Sacher and Susko, 1979).

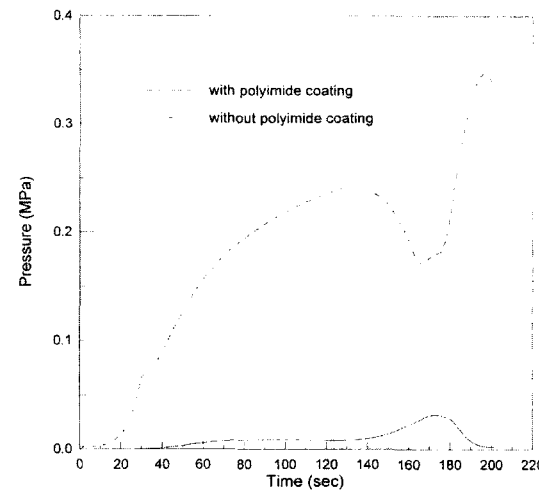

Fig. 6 Change of vapor pressures with time for the models with and without polyimide coating

Moisture flux ($\dot{m}$) into the delaminated space is given by Fick's first law as following,

$$\dot{m} = D\left(\frac{\partial C}{\partial x}\right)_{x=0} \tag{6}$$

The vapor pressure is obtained numerically by the finite difference method from Eqs. (2), (4), (6) and a steam-state equation. The detailed method for the calculation of the vapor pressure is presented at our previous study (Lee and Lee, 1999).

Fig. 6 shows the change of vapor pressures in the delaminated gap with and without polyimide, when the moisture is absorbed during 168 hours at 85℃/85%. It is concluded that the vapor pressure is very low in the case with polyimide coating and the contamination factor affects the vapor pressure little, which is different from the case without polyimide coating (Lee and Lee, 1999). It is reasonable because the polyimide coating allows low moisture absorption (Omi et al., 1991).

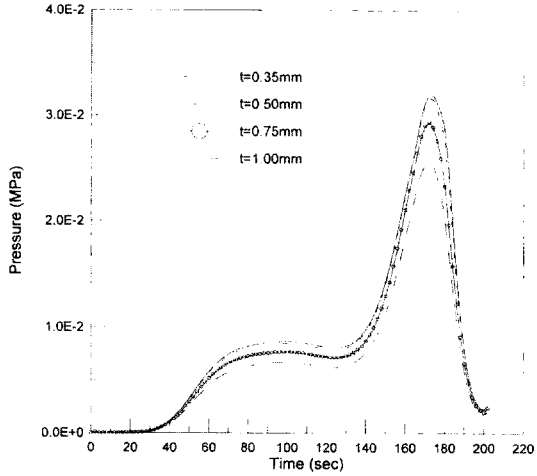

Fig. 7 Change of the calculated vapor pressure with the thickness of EMC above the chip and below the diepad in the package with polyimide coating

Fig. 7 shows the vapor pressures for various thickness of EMC above the chip and below the diepad in the package with polyimide coating. The vapor pressure increases as the thickness of EMC decreases similarly with the case without polyimide coating (Lee and Lee, 1999), but the effect is rather small.

4. Analysis of C(t)-integral Values Under Hygrothermal Loading

Because during the reflow soldering process the temperature reaches about 230℃, which is above the glass transition temperature of EMC, EMC can display a viscoelastic behavior (Kenner et al., 1997; Katouzian et al., 1995). The relation between strain rate $\dot{\varepsilon}$ and stress σ under creep is as follows,

$$\dot{\varepsilon}=A\sigma^n \tag{7}$$

where A and n are creep constants, and the values are shown in Table 4 (Katouzian et al., 1995) when the units of $\dot{\varepsilon}$ and σ are per sec and MPa, respectively.

The creep fracture mechanics parameter C(t)-integral which shows the stress intensity at the crack tip is defined in the form,

Table 4 Creep constants of EMC

	Below Tg	Above Tg
A	1.0×10^{-8}	5.0×10^{-4}
n	2.5	1.2

$$C(t)=\int_{\Gamma_\varepsilon} W_s^*=dy-T_i\left(\frac{\partial \dot{u}_i}{\partial x}\right)ds \tag{8}$$

where

$$W_s^*=\int_0^{\dot{\varepsilon}_{min}}\sigma_{ij}d\dot{\varepsilon}_{ij} \tag{9}$$

W_s^* is the strain energy rate density as the function of stress σ and strain rate $\dot{\varepsilon}$, Γ_ε is the integration contour within the creep strain rate dominant region, $T_i(=\sigma_{ij}n_j)$ is the traction vector defined by outward unit normal vector, n_j, along Γ_ε, u_i is the displacement vector, s is the length of the contour, and x, y are the rectangular coordinates which have the origin at the crack tip.

The delamination between the chip and the diepad is assumed because the differences of strains at "B" position in Fig. 3(c) are largest. We assume that the delamination is continued to "C" position along the interface between diepad and polyimide coating since the strain difference around "B" show higher values in the horizontal way than in the vertical way, and crack propagates from "C" position to polyimide coating and EMC. The QPEs (quarter point elements) are used at the crack tip (Barsoum, 1976) and surrounded by the transition elements (Lim et al., 1993) as shown in Fig. 8. The rest are modeled as the regular elements and the mesh shape which is shown in Fig. 9 is the same as that for thermal stress analysis except the neighborhood of the crack tip.

The crack direction growing from "C" position in Fig. 3(c) to polyimide coating is defined as θ_1 in Fig. 10. We use J-integral for the determination of the crack direction in the polyimide coating because the polyimide is under an elastic behavior as explained above. The crack direction is determined as that of maximum J-integral for the same crack length and vapor pressure in the range of $\theta_1=0°\sim135°$. The crack length through the polyimide is assumed 0.0254 mm and the contamination factor is assumed as 0.5. The changes

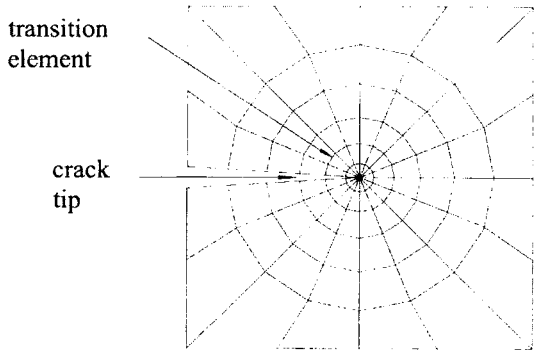

Fig. 8 Crack tip modeling for the calculation of C(t)-integral value

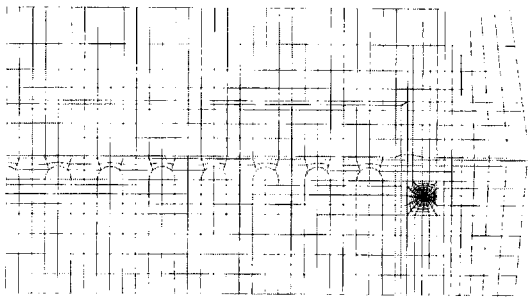

Fig. 9 FE model with the crack

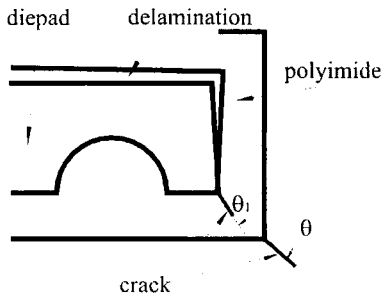

Fig. 10 Crack directions in polyimide coating and EMC

of J-integral with time are calculated with the change of crack direction. The maximum values for the time are shown in Table 5. The path independence of the J-integral is obtained in each case. It is concluded that the crack grows in polyimide in the same direction as that of delamination because the maximum J-integral is the largest for the crack direction of $\theta_1=90°$.

Next, after the crack growing in polyimide reaches the "D" position in Fig.3 (c), we assume

Table 5 Change of maximum J-integral with time with the crack direction in polyimide coating

Crack direction	Maximum J-integral (MPa mm)
0°	0.03865
45°	0.06764
67.5°	0.10490
90°	0.13650
135°	0.01846

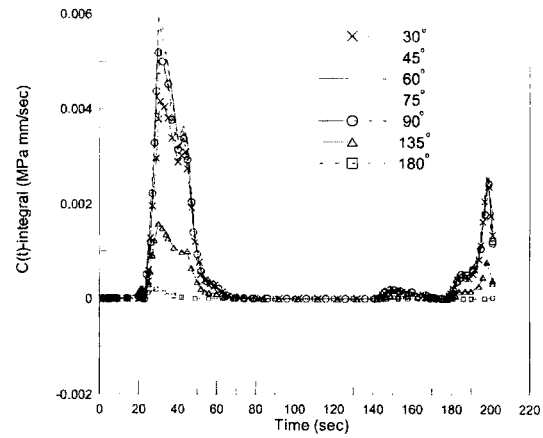

Fig. 11 Change of C(t)-integral value with the crack direction in EMC during the reflow soldering process

that the delamination is continued from "D" to "E" since "E" has higher strain difference values than other locations around "D" in Fig. 3(c) and the crack grows from "E" position into EMC. The crack direction growing from "E" position in Fig. 3(c) to EMC is defined as θ in Fig. 10. We determine the crack direction as that at which maximum C(t)-integral value for the same crack length and vapor pressure is obtained. The crack length is assumed 0.15 mm (EMC crack length/total crack length=0.034), and the contamination factor is assumed as 0.5. The change of C(t)-integral value with time is calculated for different crack directions as shown in Fig. 11. Table 6 shows that those values are ascertained to be independent of the contours of integration. For the case without polyimide coating, the vapor

pressure affects C(t)-integral value very much (Yong and Lee, 2000), but for the case with polyimide coating, the vapor pressure due to moisture is little and doesn't affect C(t)-integral value and the contamination factor doesn't affect C(t)-integral value. Fig. 11 shows that C(t)-integral value is largest at $\theta=60°$ and the crack in EMC will grow in that direction. Therefore, from now on, we will calculate C(t)-integral value for this direction.

5. Calculation of C(t)-integral Values with the Change of Design Variables Under Hygrothermal Loading

To examine how the fracture resistance changes when copper is substituted for alloy 42 as the materials of diepad and leadframe, the changes of C(t)-integral values with time are calculated and the maximum values are shown in Table 7. C(t)-integral value for the case using copper is similar to that for the case using alloy 42. Therefore, the change from alloy 42 to copper of material of diepad and leadframe is not effective in the prevention of fracture due to hygrothermal loading.

To examine the change of fracture resistance when the thicknesses of EMC above the chip and under the diepad change from 1 mm to 0.75 mm 0.5 mm and 0.35 mm, the C(t)-integral values with time are calculated and the maximum value for each case is shown in Table 8. In the package without polyimide coating, the maximum C(t)-integral value increases as the thickness of EMC decreases. On the contrary, in the package with polyimide coating, it is better to decrease the thickness of EMC, because the maximum C(t)-integral value decreases as the thickness of EMC decreases, and especially the maximum C(t) value at 0.35 mm decreases to about 11% of the value at 1 mm. Table 8 also shows that C(t)-integral values for the model with polyimide coating are smaller than those for the model without polyimide coating under hygrothermal loading and the ratio of the C(t)-integral value for the

Table 6 Maximum C(t)-integral value with time for each contour in case of crack direction of 60° in EMC

Contour number	Maximum C(t)-integral value (MPa mm/sec)
1	0.005981
2	0.005933
3	0.005950
4	0.005980
5	0.005991

Table 7 Changes of maximum C(t)-integral values with the different materials of diepad and leadframe

Material	Maximum C(t)-imtegral value (MPa mm/sec)		Ratio of maximum C(t)-integral value with and without the polyimide coating
	With polyimide	Without polyimide	
Alloy 42 (present)	0.005950	0.01343	0.443
Copper	0.005989	0.01328	0.451

Table 8 Changes of maximum C(t)-integral values with the thickness of EMC above the chip and below the diepad

Thickness of EMC (mm)	Maximum C(t)-integral value (MPa mm/sec)		Ratio of maximum C(t)-integral value with and without the polyimide coating
	With polyimide	Without polyimide	
1.00 (present)	0.005950	0.01343	0.443
0.75	0.003872	0.03116	0.124
0.50	0.001473	0.05420	0.027
0.35	0.000679	0.05901	0.012

package with polyimide coating to that without polyimide coating decreases much from 0.443 to 0.012 as the thickness of EMC decreases. Consequently, it is dangerous to reduce the thickness of EMC for the model without polyimide coating, but for the model with polyimide coating it is good to reduce the thickness of EMC for increasing the fracture resistance as well as economical benefit.

To know the effect of the ratio of the chip size to the diepad size on the fracture resistance, the C(t)-integral values are calculated with changing the chip size for the fixed diepad size, and the maximum values with time are shown in Table 9. It is helpful for the reliability of package to reduce the ratio, and it is the same tendency for the model without polyimide coating.

To examine the effect of the ratio of the chip thickness to the diepad thickness, the C(t)-integral values with time are calculated when the diepad thickness is decreased from 8 mil (0.2032 mm) to 5 mil (0.127 mm) gradually for the fixed chip thickness and the maximum values are shown in Table 10. As the diepad thickness decreases, the maximum C(t)-integral value increases continuously. Therefore, to reduce the possibility of fracture, it is good to keep the diepad thickness of 8 mil. The same tendency is observed for the model without polyimide coating.

The C(t)-integral values are calculated when the location of chip and diepad is moved from present location above and below about 0.08 mm, and the maximum values with time are shown in Fig. 12. From Fig. 12, it is noted that it is better to move up the location of chip and diepad. There may be the danger of torsion due to the large difference between the thickness of EMC above the chip and that below the diepad, if the location is changed much. Therefore it is good to move up the location of the chip and diepad a little.

To examine the effect of the dimple on the diepad on the fracture resistance, we calculated C(t)-integral values for the model with and without dimples. The full delamination is assumed to occur at the interface between diepad bottom surface and polyimide in the case of a flat diepad. This is due to the results (Adachi et al., 1993;

Table 9 Changes of maximum C(t)-integral values with the ratio of chip to diepad size

Ratio	Maximum C(t)-integral value (MPa mm/sec)		Ratio of maximum C(t)-integral value with and without the polyimidecoating
	With polyimide	Without polyimide	
0.906	0.004771	0.01297	0.368
0.938	0.005637	0.01306	0.432
0.971 (present)	0.005950	0.01343	0.443
0.986	0.006115	0.01351	0.453
1.000	0.006935	0.01387	0.500

Table 10 Changes of maximum C(t)-integral values with the ratio of chip to diepad thickness

Ratio	Maximum C(t)-integral value (MPa mm/sec)		Ratio of maximum C(t)-integral value with and without the polyimide coating
	With polyimide	Without polyimide	
2.250 (present)	0.005950	0.01343	0.443
2.483	0.006487	0.01389	0.467
2.769	0.006847	0.01460	0.469
3.130	0.007173	0.01478	0.485
3.600	0.008675	0.01564	0.555

Kitano et al., 1988 ; Fukuzawa et al., 1985) that the delamination occurs at the interface between diepad and EMC for the model of a flat diepad without polyimide coating. Fig. 13 shows the C(t)-integral values with time for the flat and dimpled diepads. It is observed that the dimpled diepad is better for fracture resistance than the flat diepad and the polyimide coating increases the reliability of package. The results are acceptable because the dimple has the role to increase the adhesive strength between the parts in general and the polyimide coating prevents moisture permeation.

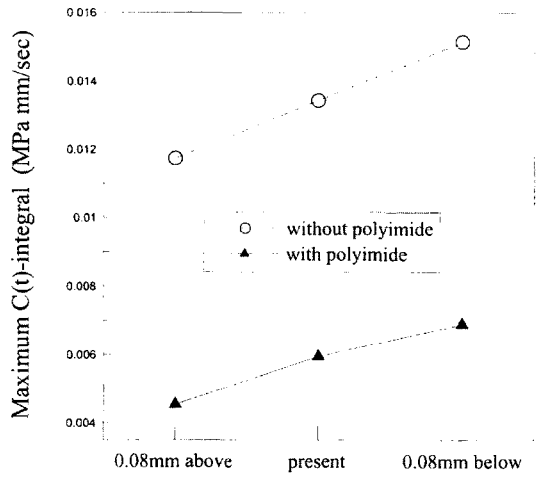

Fig. 12 Changes of maximum C(t)-integral values with the location of chip and dieqad in the package

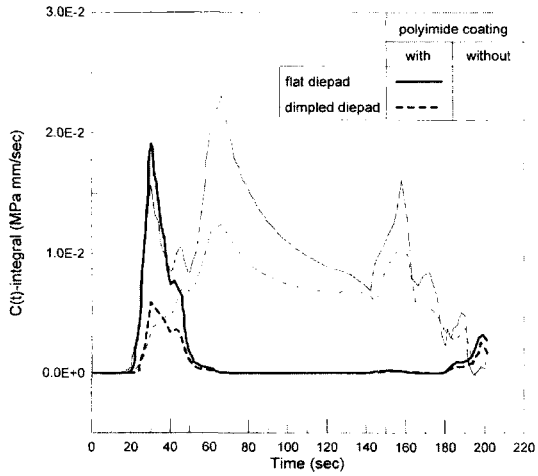

Fig. 13 Comparison of C(t)-integral values for the packages with the flat and dimpled diepads

6. Conclusions

In this paper, the delamination and crack analysis of plastic IC package with polyimide coating under thermal loading and mechanical loading due to vapor pressure in the reflow soldering process are accomplished. The location and thickness of polyimide coating to depress the possibility of delamination between the parts are obtained by viscoelastic strain analysis using finite element method (FEM), and it is clarified that the polyimide coating can decrease the maximum differences of strains at the interface.

To evaluate the reliability of the IC package, the creep fracture mechanics parameter, C(t)-integral value is calculated under hygrothermal loading with various design variables. By doing fracture mechanics analysis, the design conditions to depress the fracture were suggested. The results show that polyimide coating surrounding chip and diepad has the effect to depress the crack growth in the package in reflow soldering process by reducing C(t)-integral values. Especially, since the polyimide coating prevents the vapor pressure from occurring, the contamination factor has little effect on the vapor pressure and C(t)-integral value.

Acknowledgment

This work was supported by grant No. R01-2001-00388 from the Korea Science & Engineering Foundation. S X Zhao appreciates the support of the Brain Pool program of the Korean Federation of Science and Technology Societies.

References

Adachi, M., Ohuchi, S. and Totsuka, N., 1993, "New Mode Crack of LSI Package in the Solder Reflow Process," *IEEE Transactions on Components, Hybrids and Manufacturing Technology*,

Vol. 16, pp. 550~554.

Barsoum, R. S., 1976, "On the Use of Isoparametric Finite Element in Linear Fracture Mechanics," *International Journal for Numerical Methods in Engineering*, Vol. 10, pp. 25~37.

Fukuzawa, I., Ishiguro, S. and Nanbu, S., 1985, "Moisture Resistance Degradation of Plastic LSIs by Reflow Soldering," *Proceeding on IEEE International Reliability Physics Symposium*, pp. 192~197.

Glaser, J. C. and Juaire, M. P., 1989, "Thermal and Structural Analysis of a PLCC Device for Surface Mount Process," *ASME Transactions on Journal of Electronic Packaging*, Vol. 111, pp. 172~178.

Hattori, T., Sakata, S. and Murakami, G., 1989, "A Stress Singularity Parameter Approach for Evaluating the Interfacial Reliability of Plastic Encapsulated LSI Devices," *ASME Transactions on Journal of Electronic Packaging*, Vol. 111, pp. 243~245.

Katouzian, M., Bruller, O. S. and Horoschenkoff, A., 1995, "On the Effect of Temperature on the Creep Behavior of Neat and Carbon Fiber Reinforced PEEK and Epoxy Resin," *Journal of Composite Materials*, Vol. 29, pp. 372~387.

Kawamura, N., Kawakami, T., Matsumoto, K., Sawada, K. and Taguchi, H., 1993, "Structural Integrity Evaluation for a Plastic Package during the Soldering Process," *Proceeding on 1993 ASME International Electronics Packaging Conference*, pp. 91~95.

Kenner, V. H., Harper, B. D. and Itkin, V. Y., 1997, "Stress Relaxation in Molding Compounds," *Journal of Electronic Materials*, Vol. 26, pp. 821~826.

Kitano, M., Kawai, S., Nishimura, A. and Nishi, K., 1989, "A Study of Package Cracking during the Reflow Soldering Process," *Transactions of the Japan Society Mechanical Engineering*, Vol. 55, No. 510. pp. 356~363.

Kitano, M., Nishimura, A., Kawai, S. and Nishi, K., 1988, "Analysis of Package Cracking During Reflow Soldering Process," *Proceeding on IEEE International Reliability Physics Symposium*, pp. 90~95.

Kornblum, Y. and Glaser, J. C., 1989, "Combined Moisture and Thermal Stresses Failure Mode in a PLCC," *ASME Transactions on Journal of Electronic Packaging*, Vol. 111, pp. 249~254.

Kuo, A. Y., Chen, W. T., Nguyen, L. T., Chen, K. L. and Slenski, G., "Popcorning — A Fracture Mechanics Approach," *Proceedings on 46th Electronic Components and Technology Conference*, pp. 869~874.

Lee, K. Y. and Lee, T. S., 1999, "Hygrothermal Fracture Analysis of Plastic IC Package in Reflow Soldering Process," *ASME Journal of Electronic Packaging*, Vol. 121, pp. 148~155.

Lim, I. L., Johnston, I. W. and Choi, S. K., 1993, "Application of Singular Quadratic Distorted Isoparametric Elements in Linear Fracture Mechanics," *International Journal for Numerical Methods in Engineering*, Vol. 36, pp. 2473~2499.

Nguyen, L. T., 1993, "Reliability of Postmolded IC Packages," *ASME Journal of Electronic Packaging*, Vol. 115, pp. 346~355.

Omi, S., Fujita, K., Tsuda, T. and Meade, T., 1991, "Causes of Cracks in SMD and Type-Specific Remedies," *Proceeding on Electronic Components Conference*, pp. 766~771.

Romer, B. and Pape, H., 1989, "Stress Effects of Package Parameters on 4MEGA DRAM with Fractional Factorial Designed Finite Element Analysis," *Proceeding on Electronic Components Conference*, pp. 832~839.

Sacher, E. and Susko, J. R., 1979, "Water Permeation of Polymer Films. I. Polyimide," *Journal of Applied Polymer Science*, Vol. 23, pp. 2355~2364.

Sauber, J., Lee, L., Hsu, L. S. and Hongsmatip, T., 1994, "Fracture Properties of Molding Compound Materials for IC Plastic Packaging," *Proceeding on 44th Electronic Components and Technology Conference*, pp. 164~170.

Stevens, K. K., Wong, T. L., Renavikar, A. and Chen, W., 1990, "Fracture of Glass Seals in Surface Mount IC Packages," *ASME Transactions on Journal of Electronic Packaging*, Vol. 112, pp. 162~167.

Takeuchi, E., Takeda, T. and Hirano, T., 1990, "Effect of Combination between Various Polyimide Coating Materials and Molding Com-

pounds on the Reliability of Integrated Circuits (ICs)," *Proceeding on Electronic Components Conference*., pp. 818~823.

Tay, A. A. O. and Lin, T. Y., 1996, "Effects of Moisture and Delamination on Cracking of Plastic IC Package During Solder Reflow," *Proceeding on 46th Electronic Components and Technology Conference*, pp. 777~782.

Yang, J. H. and Lee, K. Y., 2000, "Cracking Analysis of Plastic IC Package in Consideration of Viscoelasticity," *Proceeding on 3rd Electronics Packaging Technology Conference*, pp. 251~257.